Do flame describing functions suitably represent combustion dynamics under self-sustained oscillations?

Preethi Rajendram Soundararajan, Guillaume Vignat, Daniel Durox, Antoine Renaud, Sébastien Candel

Do flame describing functions suitably represent combustion dynamics under self-sustained oscillations?

Preethi Rajendram Soundararajan[1], Guillaume Vignat[2], Daniel Durox[3], Antoine Renaud[4], Sébastien Candel[5]

Laboratoire EM2C, CNRS, CentraleSupélec, Université Paris-Saclay, 3 rue Joliot Curie, 91190 Gif-sur-Yvette, France

Abstract

Transfer function concepts that appear in many areas and most notably in control systems have been extensively used to represent the flame response in low-order models of combustion instability. Much of the theoretical work is based on flame transfer functions (FTF). In recent years, the nonlinear extension of FTF, namely the flame describing function (FDF), has been used to get a more accurate representation of the flame response when the level of oscillation becomes large and the system reaches a limit cycle. Despite their wide use, the validity of using FTF/FDF to represent flame response still remains to be experimentally substantiated. This article is aimed at providing a direct assessment of the capacity of the FDF to suitably describe the flame behavior under self-sustained oscillations (SSO) for a spray-swirl flame anchored by an injector that is weakly-transparent to acoustic waves. This is accomplished by making use of an experimental combustion configuration that not only exhibits unstable oscillations but also features a set of driver units to modulate the flame (namely open-loop modulation or OLM). The flame is modulated at the frequency of SSO, and the amplitude of incident velocity modulations is then progressively varied until it coincides with that found under SSO. The injector dynamics is shown to be different between SSO and OLM for an injector that is weakly-transparent to acoustic waves and imposes a certain degree of decoupling between plenum and chamber. For such injectors, the FDF built with the upstream velocity would not suitably represent SSO as this lumps the injector and flame dynamics together. It is then important to consider velocity measurement at the injector outlet at a point where the relative velocity fluctuation matches the relative volumetric flow rate fluctuation. The describing function with velocity reference at the injector outlet is measured for various input levels and found to approximately match those measured under SSO. The best match is obtained when the amplitude of external modulation induces a level of velocity oscillations closest to that prevailing under SSO. This demonstrates that the FDF may suitably capture the nonlinearity of the flame response, at least in the configuration investigated in this research.

Keywords: Combustion dynamics, flame transfer/describing function, limit cycle oscillations, injector dynamics, acoustically weakly-transparent injectors.

1. Introduction

This article is dedicated to the memory of Professor J.E. Ffowcs Williams (also known to many of his colleagues and friends as Shôn). Shôn was an influential and brilliant scientist. He contributed quite

[1]Corresponding author: preethi.rajendram-soundararajan@centralesupelec.fr

[2]guillaume.vignat@gmail.com. Present address: Stanford University, Department of Mechanical Engineering, Stanford, CA 94305, USA.

[3]daniel.durox@centralesupelec.fr

[4]antoine.renaud@centralesupelec.fr

[5]sebastien.candel@centralesupelec.fr

extensively to aeroacoustics, the science of noise generated aerodynamically. He was also one of the early proponents of anti-sound, the reduction of sound by cancelation with secondary sources of sound. Of course, there were discussions and even experimental demonstrations of this concept, but FW understood that active noise control could become a reality by making use of advances in adaptive beamforming and optimal control [1]. FW also considered that similar concepts could be used to control unstable flows, and the principles of sound cancellation implemented in noise control technology could be extended in that direction [2]. He worked out some speculative examples like those of controlling the Kelvin-Helmholtz instability of shear layers or the gravitational instability of stratified fluids [3], and also investigated more practical possibilities like that of suppressing rotating stall and surge instabilities in compressors [2]. FW cited the progress made in the control of combustion instabilities demonstrated in simple devices exhibiting a single mode of instability and later on in the suppression of acoustically coupled instability in larger scale experiments on reheat "buzz"[4]. Work in this direction was notably pursued by one of his students, and later colleague, Ann Dowling [5, 6] and her own doctoral students. After many early experiments in active control of combustion, it became clear that progress could only be made by developing modeling methods [7–11], and this gave rise to a considerable research effort that was aimed at representing the combustion system and controller in the framework of control systems theory. The central idea was to describe the combustion response in terms of transfer functions, use closed-loop representations of the coupling that was achieved by acoustic modes and controller actions. Much effort has been devoted to deriving models that may guide the analysis of combustion dynamics phenomena and may then be used as predictive tools. This modeling effort was initiated during the early days of rocket engine development where instability problems were encountered, inducing some spectacular failures [12–18]. More recently, attention has been focused on dynamical phenomena in gas turbine combustors operating in the premixed mode and using swirling flows to anchor the flames at a distance from the injection units [9, 19–29]. The present article addresses a central modeling issue in the context of swirl stabilized flames. Is it possible to suitably describe the combustion response in terms of transfer functions or their nonlinear extension, describing functions? In other words, can one model a complex multi-dimensional flow characterized by the presence of multiple scales, those of turbulence and combustion, and the fast kinetics of strongly exothermic reactions in terms of low-order dynamical tools relying on transfer or describing functions? Do these reduced descriptions capture the three-dimensional flame dynamics that are involved in the process? This analysis aims to provide direct experimental proof that transfer functions and their describing functions extensions represent the flame behavior and that the reduced-order model suitably describes the multi-dimensional reality. It is not our intention to give a general answer to the questions raised previously and the analysis is restricted to a case that has much practical importance, that of swirling flames that are compact with respect to the acoustic wavelength of the coupling modes. This case will be investigated experimentally to highlight the difficulties and limitations of this kind of representation and provide some insight on issues of low order modeling of combustion instabilities.

At this point, it is worth briefly reviewing the state of the art in low-order modeling to place the present investigation in perspective. The early analysis of combustion instability relied on the sensitive time lag (STL) theory. The flame response was represented in terms of an interaction index n and a time delay τ that was assumed to be a function of the state variables in the combustion region [12, 14, 15]. In general, these two terms were considered as parameters that could be varied to determine regions of instability. This kind of model assumed, in essence, that a transfer function existed between the state variable disturbances and combustion disturbances such as those of the heat release rate. The gain of this transfer function was a constant $G_F(\omega) = n$ while the phase was a linear function of the angular frequency $\varphi_F = \omega\tau$. More recently, considerable effort was expanded to understand mechanisms controlling instabilities and to represent the flame dynamics in terms of transfer functions. This effort is reviewed for example, in [26, 30–32]. The transfer function was introduced to link relative fluctuations of heat release rate in the flame, treated as an output, to the relative fluctuation in volume flow rate. When the relative velocity fluctuation and the mean velocity at the input are uniform, it is possible to consider that the relative volume flow rate is equal to the relative velocity fluctuation. For experimental convenience, velocity fluctuation is then considered as the input instead of volume flow rate fluctuation. The transfer function may have multiple inputs, and in the present case, one other input could be the perturbations in equivalence ratio. For the case considered in

this article, the mode of combustion is quasi-premixed, and the primary input is the disturbance in velocity (representing the disturbance in volume flow rate). The transfer function is given by

$$\mathcal{F}_0(\omega) = \frac{\dot{Q}'(\omega)/\overline{\dot{Q}}}{u'/\overline{u}} = G_F(\omega)e^{\mathrm{i}\varphi_F(\omega)} \tag{1}$$

Transfer functions were introduced, in particular, to derive active control methods and help interpret their experimental demonstrations. Transfer function expressions were obtained for many simple flames like premixed conical and "V" flames and for swirling premixed flames [33–43] and were compared in some cases with experimental data. It was then recognized that the flame response depended not only on frequency but also on the amplitude of oscillation. This led to the replacement of FTF by a describing function, i.e., a family of transfer functions with each of these functions depending on the amplitude of the input.

$$\mathcal{F}(\omega, u') = \frac{\dot{Q}'(\omega, u')/\overline{\dot{Q}}}{u'/\overline{u}} = G_F(\omega, u')e^{\mathrm{i}\varphi_F(\omega, u')} \tag{2}$$

This was employed for example in a theoretical analysis of the dynamics of a ducted flame by Dowling [44], which indicated only a gain saturation with the amplitude of velocity fluctuation. The concept of flame describing function (FDF) was generalized by Noiray et al. [45] to also consider phase dependence with respect to the amplitude of perturbations. The FDF was shown to provide an understanding of many nonlinear features observed experimentally, like frequency shifting during oscillation growth, mode switching (frequency jumping during oscillation), instability triggering, and hysteresis. With respect to the transfer function, the FDF allowed to render some of the complex behavior of practical systems and more specifically those linked to finite amplitude oscillations [46]. This has been a considerable advance because the describing function allowed to retrieve nonlinear dynamical features [47–60]. Models using the FDF yield amplitude-dependent results that allow direct comparisons with experimental data since most instability experiments are carried out when the oscillations are established and have a finite value. It was, however, found that the FDF has shortcomings and cannot easily handle complex limit cycles sustained by multiple modes. Despite these difficulties, the FDF accounts for some essential nonlinear features. It is then interesting to use this concept and see if it is representative of the combustion dynamics under self-sustained oscillations (SSO). This question is represented schematically in Fig. 1(a) and (b).

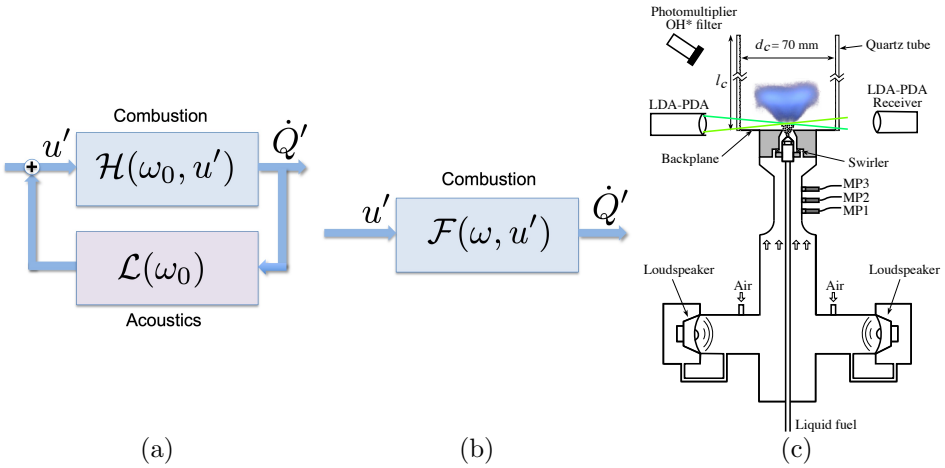

Figure 1: (a) Closed loop representation of a self-sustained instability at an angular frequency ω_0 and an amplitude of oscillation u'. The function $\mathcal{H}$ represents the flame response in the self-sustained oscillation. (b) Open-loop determination in terms of a flame describing function $\mathcal{F}(\omega, u')$. (c) Schematic of the experimental setup SICCA-Spray.

This diagram shows on the left a representation of the system when it is executing SSO and features a limit cycle at an angular frequency ω_0. The flame dynamical response is $\mathcal{H}(\omega_0, u')$. The inclusion of u' in

this expression is to indicate that the flame behavior is also controlled by the level of incident disturbances. In the center, the diagram shows the combustor being modulated externally to measure the FDF designated as $\mathcal{F}(\omega, u')$. For this measurement, one has to reduce the acoustical coupling so that the system operates in a steady regime. In practice, this may be accomplished by changing the combustion chamber size to move the resonant frequencies out of the range of interest manifested under SSO. One may then see if

$$\mathcal{F}(\omega_0, u') \simeq \mathcal{H}(\omega_0, u') \tag{3}$$

A good match between these two functions will indicate that a low-order model using a measured FDF may suitably represent the real system and will provide reasonable predictions of SSO. However, one cannot be certain that the flame behavior has not been modified when the loop is closed and when a strong acoustic coupling takes place. A modification of this type is not considered in control systems where the transfer function or describing function of the "plant" does not depend on the feedback path. Here the situation is different because the flame is a result of a complex flow where exothermic reactions take place. The dependence on amplitude of the FDF captures some of the modifications in flame dynamics, but there are perhaps other changes that arise under SSO but are not accounted for by the FDF.

This article begins with a presentation of the experimental setup (section 2). Flame dynamics are then examined using OH^* chemiluminescence images in section 3 under SSO and compared to those corresponding to external modulation (referred to as open-loop modulation or OLM). A comparison between the flame response $\mathcal{H}$ and the FDF $\mathcal{F}$ is then carried out in section 4. This is followed by section 5 that is focused on the injector dynamics under SSO and OLM. It is shown in that section that the injector operates in a different manner when the system is modulated from upstream and when the system executes self-sustained oscillations with some important consequences.

2. Experimental set-up

Experiments are carried out in a generic single injector set-up (SICCA-Spray). This configuration, shown schematically in Fig. 1(c), comprises a plenum, a swirl-spray injector, and a cylindrical chamber. Liquid heptane fuel is delivered as a hollow cone spray by a simplex atomizer producing a dispersion of fine fuel droplets. The mass flow rate of fuel is set by a Bronkhorst CORI-flow controller with a relative accuracy of 0.2%. The air flow rate measured by a Bronkhorst EL-FLOW mass flow controller with a relative accuracy of 0.6% is injected at the bottom of the plenum. The stream of air enters the chamber through an injection unit described in detail in a recent publication [61]. This unit comprises an air distributor leading to a tangential swirler with six channels. This element induces a clockwise rotation of the flow. The air and the fuel spray are delivered to the combustor through a conical section having an 8 mm diameter outlet. A swirler, designated as 716, is used in the present investigation. The swirl number determined experimentally by integrating the velocity profiles at the outlet of the injector at a height of 2.5 mm above the backplane is S=0.70 (refer to [61] for swirler characteristics). The burner is operated at a global equivalence ratio of $\phi = 0.95$ which corresponds to an airflow rate of $2.3\,\mathrm{g\,s^{-1}}$ and a fuel flow rate of $520\,\mathrm{g\,h^{-1}}$. The combustion chamber is formed by a fully transparent cylindrical quartz tube providing complete optical access to the combustion zone. Self-sustained oscillations of the system are obtained by varying the chamber length l_c. One obtains in this way different resonant frequencies and amplitudes of longitudinal limit cycle instabilities. During the measurement of FDFs under OLM, a chamber length of $l_c = 150$ mm is chosen to operate the system under stable conditions. For these measurements, two driver units located at the bottom of SICCA-Spray are excited to achieve different levels of fluctuations. These driver units are modulated at the same frequencies as those of SSO and at an amplifier voltage that is close to the level of relative fluctuations observed under SSO. When the system is operating under SSO, the driver units are left inactive.

2.1. Diagnostics

The SICCA-Spray experimental setup comprises three microphones plugged on the plenum, designated as MP1, MP2, and MP3 in Fig. 1(c). These sensors are Brüel & Kjær 4938 microphones mounted with type 2670 preamplifiers having a relative accuracy of 1% and a passband frequency set between 15 Hz and 20 kHz. Apart

from the measurement of pressure signals, these microphones are also used to determine the acoustic velocity fluctuations with the two-microphone method [62]. Velocity fluctuations in the chamber are measured with a Dantec two-component phase Doppler anemometer (PDA). This measurement is directly obtained on the spray of heptane droplets. To have the best attainable data rate, the measurements are performed with the system configured exclusively for anemometric measurements (laser Doppler anemometry, LDA), which allows only for the evaluation of axial velocity from heptane droplets. Details on the velocity measurement location is given in section 2.2. The transmitting optics of the system produces a 532 nm laser beam that is split in two by a Bragg cell. The focal length of the transmitting optics is 500 mm and that of the receiving optics is 310 mm. The theoretical size of the laser beam intersection as viewed by the receiving optics is 0.14 $\times$ 0.14 $\times$ 0.23 mm.

An estimate of heat release rate (HRR) integrated over the flame volume is obtained by measuring the OH^* chemiluminescence (with a 10 nm filter centered at 308 nm) from the flame using a photomultiplier tube. The validity of using OH^* chemiluminescence as HRR indicator has been systematically validated in the current configuration in [63]. The spray flame considered in this study is found to operate in a quasi-premixed fashion due to the recessed position of the atomizer in the injector. This positioning allows a part of the fuel spray to impinge on the conical section of the injector nozzle, which fluctuates along with the air flow. The equivalence ratio fluctuations therefore remain low at the injector outlet compared to the velocity fluctuations and there is no significant spatial stratification in the flame zone. The readers are referred to [63] for the detailed analysis. Additionally a PI-MAX intensified CCD camera from Princeton Instruments is used to obtain the flame images. The signals from the plenum microphones and photomultiplier are sampled simultaneously during the velocity measurements by the LDA system for a period of 10 s and at a data rate of roughly 25,000 Hz.

2.2. Velocity measurement location

The velocity measurements for the determination of FDF (given by Eq. 2) is obtained at the injector outlet using LDA. When using a swirling injector, the velocity at the exit of the injector is nonuniform and this raises a question on choosing an optimal position for the measurement. Normally FDFs are defined, in the absence of equivalence ratio fluctuations, as the ratio of relative heat release fluctuations to the relative volumetric flow fluctuations $(\dot{q}'_v/\overline{\dot{q}}_v)$. However, from a practical viewpoint it is difficult to measure relative volumetric flow rate fluctuation and this quantity is generally replaced by the relative velocity fluctuation as in Eq. (2). This defines a condition for determining the reference position for velocity measurements; one must choose a location at the exit of the injector where the relative velocity fluctuation coincides with the relative volumetric flow rate fluctuation. The measurements and the subsequent determination of this location are detailed in [63]. For the swirler 716, the reference position for the measurement of velocity is located at a distance of $r = 4$ mm from the center of the injector and at a height of $h = 2.5$ mm from the backplane. The measured axial velocity at the exit of the injector is henceforth referred to as $u_{c,r}$. At the reference position, the mean droplet size of heptane spray is 4.5 µm and hence it can be reasonably assumed that the droplet velocity at this point is equivalent to the flow velocity.

3. Flame dynamics

Before examining the FDF and the flame response in terms of gain and phase, it is beneficial to compare the flame dynamics under SSO and OLM using OH^* chemiluminescence images as presented in Fig. 2. The images are captured by a PI-MAX intensified camera equipped with a Nikon 105 mm UV lens and an Asahi optical bandpass filter (10nm centered at 310 nm corresponding to emission bands of OH* radicals in the flame). The camera is triggered with respect to the instability using the photomultiplier signal, which is low pass filtered with a cut-off frequency of 800 Hz using an analog filter. This improves triggering by reducing the jitter present in the photomultiplier signal. A Tektronix TBS 2000 oscilloscope provides a trigger signal when the filtered photomultiplier signal reaches its mean value and at its rising edge. This setup is used to obtain the phase averaged flame images shown in Fig. 2. The exposure is 40 µs long. The images of Fig. 2 are averaged over 1000 individual samples and processed with an Abel inversion algorithm.

For the measurements, the quartz tube for the unstable case is 265 mm long and the limit cycle features a frequency of 533 Hz. The amplitude of velocity oscillation at $(r, z) = (4.0, 2.5)$ mm measured using LDA is $u'_{c,r}/\overline{u}_{c,r} = 9\%$, and that of the chemiluminescence signal is $I'_{\mathrm{OH}^*}/\overline{I_{\mathrm{OH}^*}} = 28.9\%$. Here and henceforth, the notation $(\cdot)$' refers to the root mean square (RMS) fluctuations, and $\overline{(\cdot)}$ refers to the mean of a quantity. The flame dynamics under SSO is shown in Fig. 2(a) and open-loop forcing is examined in Fig. 2(b-d). In Fig. 2(b), directly underneath the SSO images, the forcing level is set to match the conditions encountered under SSO. In Fig. 2(c), the forcing level is significantly lower, while in Fig. 2(d), it is significantly higher.

Figure 2: Phase-averaged, Abel-transformed flame images shown in false colors. Light intensity of OH* chemiluminescence is obtained at different phase instants of the acoustic cycle using an intensified camera. (a) Images obtained under self-sustained oscillations (SSO) at a frequency $f_0 = 533$ Hz. $I'_{\mathrm{OH}^*}/\overline{I_{\mathrm{OH}^*}} = 28.9\%$. (b-d) Images corresponding to open-loop modulation (OLM) at the frequency determined under SSO. (b) The forcing amplitude matches that observed during SSO ($I'_{\mathrm{OH}^*}/\overline{I_{\mathrm{OH}^*}} = 30.4\%$). (c) The forcing amplitude is lower than that observed during SSO ($I'_{\mathrm{OH}^*}/\overline{I_{\mathrm{OH}^*}} = 14.2\%$). (d) The forcing amplitude exceeds that observed during SSO ($I'_{\mathrm{OH}^*}/\overline{I_{\mathrm{OH}^*}} = 37.8\%$). (e-g) Flame isocontours determined by Otsu thresholding method for SSO and three levels of OLM (same, lower, and higher fluctuation level compared to SSO).

The set of images in (a) and (b), indicate that the flame shapes corresponding to SSO agree with those of OLM at 3.5 V i.e., when the velocity fluctuation levels match. On comparing SSO with OLM at other amplifier voltages where the velocity fluctuations do not match, some minor differences can be observed in

the flame shapes and intensity levels. A periodic elongation and widening is visible in all the cases starting from $\Phi = {}^{3\pi}/_{2}$ and extending till ${}^{\pi}/_{2}$, the latter corresponding to the broadest flame during the cycle. To further understand the similarities and differences between SSO and OLM, the flame front location is identified by applying the Otsu thresholding method to the OH^* images, as demonstrated by [64], and is shown in Fig. 2(e-g) when the flame is under SSO (in black) and for the four cases of OLM: same (red), lower (magenta), and higher (blue) relative intensity fluctuation compared to SSO. The extracted flame contour data evidently show a close match between the SSO and OLM flame shapes and intensity when the forcing level of OLM (i.e., at $V_0 = 3.5\,\mathrm{V}$) matches the oscillation level of SSO. At the other two OLM levels, visible differences can be observed in the flame contour shape at certain parts of the cycle. For instance, this difference is more pronounced for the higher fluctuation level between the phase instants $\Phi = {}^{\pi}/_{4}$ and ${}^{3\pi}/_{4}$. For the remaining part of the cycle, the difference is minor, with only some observable deviation close to the base of the flame. The difference in the flame contour position between SSO and OLM is more prominent for the lower amplitude case at all the phase instants, except at $\Phi = {}^{7\pi}/_{4}$, where the contours corresponding to all four cases almost collapse.

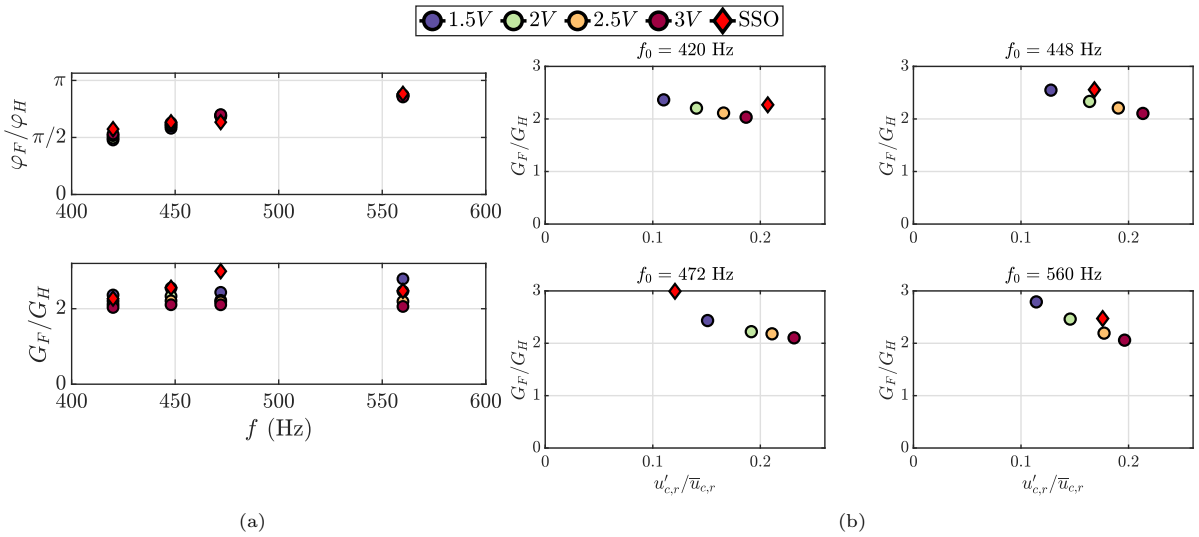

Figure 3: Comparison between the open loop describing function $\mathcal{F}$ and the combustion response under SSO, $\mathcal{H}$. (a) Phases φ_F and φ_H and gains G_F and G_H plotted at the four resonance frequencies and at different amplitude levels for OLM. The red diamonds represent phases and gains of $\mathcal{H}$ during SSOs for different chamber lengths. The circles correspond to the measured $\mathcal{F}$ during OLM obtained while modulating the flame at the SSOs frequencies. The colors pertain to four different levels of amplifier voltages (1.5, 2, 2.5, and 3 V). (b) Gain of $\mathcal{F}$ and modulus of $\mathcal{H}$ plotted as a function of the relative velocity fluctuation. The velocity is measured at the reference position $(r, z) = (4.0, 2.5)$ mm. The representation in terms of amplifier voltages shown in (a) is expressed in terms of velocity fluctuation levels in (b).

4. Comparison of FDF and flame response under limit cycle oscillations

The comparison between FDF $\mathcal{F}$ and the flame response $\mathcal{H}$ is shown in Fig. 3(a) in terms of gain and phase. For the measurements under SSO, the chamber length l_c is varied to obtain sustained oscillations at different frequencies. Chamber lengths of 250, 300, 315, and 350 mm are used to attain the oscillations at frequencies 560, 472, 448, and 420 Hz respectively. The measurement under OLM is performed by modulating the flame using the two driver units mounted upstream of the injectors at the frequencies of SSO and at four different levels of amplifier voltages (1.5, 2, 2.5, and 3 V) fed to the driver units. Although a representation based on amplifier voltage is not physically relevant, it is provided here as a common ground for OLM between flame image measurement (shown in Fig. 2) and the measurements performed to obtain the describing functions shown in Fig. 3. A representation in terms of amplifier voltage can alternatively be indicated in terms of relative velocity fluctuations, as shown in Fig. 3(b).

On comparing the phase of $\mathcal{F}$ at different fluctuation levels (Fig. 3(a) top), it can be seen that there is no discernible nonlinearity with respect to the level of fluctuation and the phases of $\mathcal{F}$ and $\mathcal{H}$ match quite well. The role of phase on stability analyses (see for example [32, 45]) is critical, and the experimentally observed match validates the usage of FTF/FDF in reduced-order models. Contrary to the phase observation, one may notice the presence of nonlinearity in the gain of OLM (Fig. 3(a) bottom) with respect to the fluctuation level at all the frequencies. Fig. 3(b) shows the gain G_F as a function of velocity fluctuation levels at the four frequencies considered in this study along with G_H. At $f_0 = 448\,\text{Hz}$ and $560\,\text{Hz}$, the fluctuation levels match between SSO and OLM at an amplifier voltage of $2\,\text{V}$ and $2.5\,\text{V}$ respectively, where one may also notice that the gains G_F and G_H match in these two cases. Whereas, at $f_0 = 472\,\text{Hz}$ and $420\,\text{Hz}$ none of the OLM cases matches with the fluctuation level of SSO. Hence, a match of gain between OLM and SSO is not attained, but the respective values are close. These results and the flame images shown in Fig. 2 clearly indicate the importance of utilizing $\mathcal{F}$ that matches with the velocity fluctuation level of $\mathcal{H}$ in the low-order models to have a good prediction of instabilities. If the low-order model uses a $\mathcal{F}$ that does not match the level of SSO, one might still be able to potentially predict whether or not the system will be unstable purely based on the phase information from the FDF. But the prediction of limit cycle amplitude would potentially be erroneous due to the mismatch in gain.

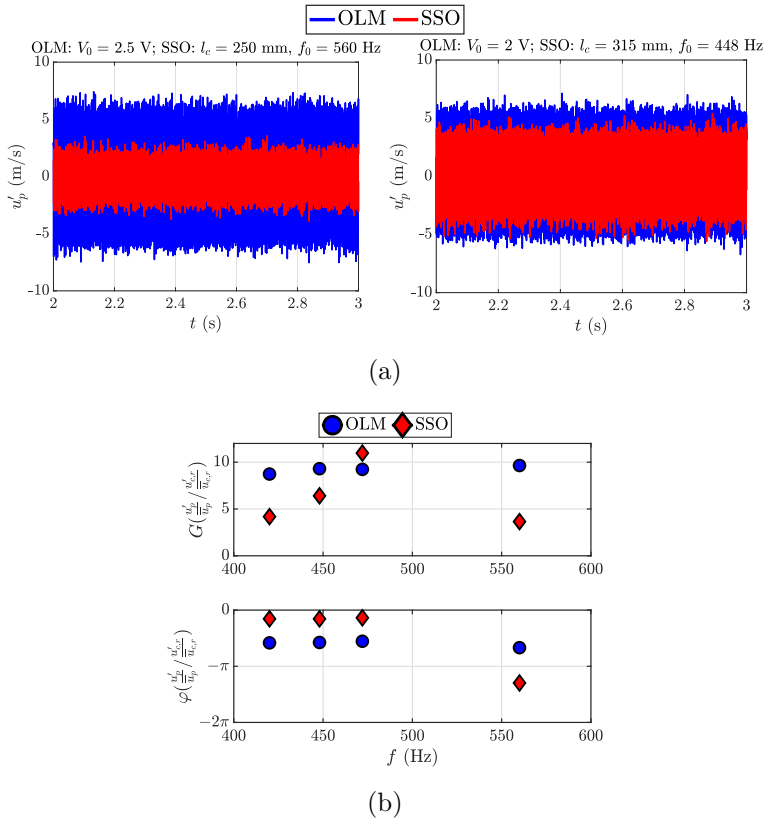

Figure 4: (a) Comparison of time evolution of plenum velocity between an OLM and SSO shown for a period of 1 s for the chamber lengths $l_c = 250\,\text{mm}$ and $315\,\text{mm}$. Results are plotted when the chamber velocity fluctuation level of OLM matches with that of SSO. (b) The gain and phase of relative plenum velocity fluctuations to relative chamber velocity fluctuations. At $f_0 = 448\,\text{Hz}$ ($l_c = 315\,\text{mm}$) and $560\,\text{Hz}$ ($l_c = 250\,\text{mm}$), the results are shown when the chamber velocity fluctuations of OLM coincide with those of SSO. At $f_0 = 420\,\text{Hz}$ ($l_c = 350\,\text{mm}$) and $472\,\text{Hz}$ ($l_c = 300\,\text{mm}$), the results are shown when the chamber velocity fluctuations of OLM are closest to SSO.

5. Injector dynamics during SSO and OLM

Although the FTF/FDF framework considers the reference velocity at the base of the flame, it is a common practice to use a velocity reference for the transfer function in the plenum, upstream of the injection unit (this is exemplified in [50], and more recently by [65, 66]). This choice is made because of the practical difficulties associated with the measurement of velocity at the base of the flame, which would mandate some form of optical measurement technique to access the flame zone. For an acoustically transparent injector, using the upstream velocity would still be valid as the injector dynamics would be the same between SSO, where there is strong pressure oscillation downstream, and during modulation of the flame from upstream. However, the injector considered in the present work is only weakly transparent to acoustic waves due to the high pressure drop and abrupt area changes in the swirler channels. This raises a question on whether the FDF measured with a reference velocity in the plenum and an upstream acoustic modulation would suitably represent the flame dynamics during SSO. Figure 4(a) shows the time evolution of plenum velocity between OLM and SSO when the chamber velocity $u'_{c,r}$ coincides in these two cases. The plenum velocity is obtained by the two-microphone method from the pressure signals of the plenum microphones MP1 and MP3 (refer Fig. 1(c)). Chamber velocity is measured by LDA as described in section 2. Figure 4, left shows the plenum velocity during an SSO at $l_c = 250\,\text{mm}$ and OLM at $V_0 = 2.5\,\text{V}$, and on the right is the SSO at $l_c = 315\,\text{mm}$ and OLM at $V_0 = 2\,\text{V}$. It can be seen that for the same level of velocity fluctuations in the chamber, OLM always yield a higher level of plenum velocity u'_p than SSO. This means that the amplitude of the relative velocity fluctuation in the plenum is not preserved between SSO and OLM. Figure 4(b) shows the gain and phase of relative velocity fluctuations in the plenum to the relative velocity fluctuations in the chamber at different frequencies considered in this study. The data plotted at $f_0 = 448\,\text{Hz}$ and $560\,\text{Hz}$ correspond to a situation where the chamber velocity fluctuations nearly coincide for SSO and OLM. At $f_0 = 420\,\text{Hz}$ and $472\,\text{Hz}$, the data points pertain to a situation where the relative velocity fluctuations in the chamber of OLM are closest to the SSO case but do not quite match. Significant differences can be observed between SSO and OLM with regard to the velocity fluctuation ratio, with the gain during OLM being twice as high as that corresponding to SSO for most frequencies, except at $472\,\text{Hz}$, where this difference is minor. It is also found that under OLM, the phase between plenum and chamber velocity fluctuations remains the same at all frequencies and is slightly higher than $\pi/2$. However, when the system is under SSO, the phase is rather close to 0 at lower frequencies and close to $-\pi$ at $560\,\text{Hz}$. Gaudron et al. [67] also observe such differences in the dynamical state of a swirling injector system between upstream and downstream modulation but the reasoning for this was not well detailed. A downstream modulation can be considered a state similar to SSO, where there is pressure oscillations downstream. A measurement performed upstream of the injector would, in fact, lump the injector and flame dynamics together and will not suitably represent the flame dynamics under SSO. Thus, for an injector that is weakly-transparent to acoustic waves, the velocity measurement for FDF determination should be positioned at the injector outlet. Additionally for a swirling injector, the chosen location at the injector outlet should be such that the relative volumetric fluctuations coincide with the relative velocity fluctuations to be suitably used in the FDF framework.

6. Conclusion

Although many theoretical models in combustion instability rely on transfer functions or describing functions, it was essential to see if these concepts are effectively applicable, and in particular, if they can be used in the case of complex turbulent spray flames formed by swirling injectors. This central question is investigated by comparing two situations: the first corresponding to a well-established limit cycle self-sustained oscillation (SSO), while the second could be assimilated to an open-loop modulation (OLM) in which the flame is externally modulated. Three levels of external modulation are chosen—same, lower, and higher levels than the SSO fluctuations. It is shown that the flame dynamics observed using Abel-transformed OH^* light intensity images matches best when the level of acoustic oscillation in the two situations are equal. It is then found that the gain of the flame describing function (FDF) is close to that of the flame response measured under SSO, when the level of oscillation in the externally modulated flame (OLM) equals that found under SSO. The level of fluctuation does not affect the phase, and all the OLM cases match with the

SSO tests. These elements confirm that the FDF framework is applicable and that it is crucial to consider the dependence of flame response on the level of incident perturbations. Additionally, it is shown that the injector dynamics during OLM and SSO is not the same for the case of an injector that is weakly-transparent to acoustic waves. It is advisable to use the chamber velocity for FDF determination, since the use of plenum velocity would lump the dynamics of injector and flame together and not represent the flame dynamics under SSO. The FDF obtained with plenum velocity would neither have the correct gain nor the correct phase evolution, and it would not be possible to predict the unstable operating points with low-order models. The present experiments although restricted to a specific case provide a validation of the FDF concept in the analysis of combustion instabilities leading to limit cycle oscillations.

Acknowledgments

This article is dedicated to the memory of Shôn Ffowcs Williams. One of us (SC) had the privilege to meet Shôn at an early stage. After a seminar in Cambridge, Shôn drove SC on small British country roads from Cambridge to Bristol to participate to the "Noise panel" while discussing aeroacoustics, noise from entropy spots traveling through nozzles and turbines, and many other issues. SC has kept vibrant memories of this initial encounter with an admirable scientist. The present work benefited from the support of project FASMIC ANR16-CE22-0013 of the French National Research Agency (ANR) and of the European Union's Horizon 2020 research and innovation programme, Annulight with grant agreement no. 765998.

References

[1] J. Ffowcs-Williams, Review lecture: Anti-sound, Proc. Royal Soc. A: Mathematical, Physical Eng. Sci. 395 (1984) 63–88. doi:doi.org/10.1098/rspa.1984.0090.
[2] J. Ffowcs-Williams, M. Harper, D. Allwright, Active stabilization of compressor instability and surge in a working engine, J. Turbomachinery 115 (1993) 68–75. doi:doi.org/10.1115/1.2929219.
[3] J. Ffowcs-Williams, Active flow control, J. Sound Vib. 239 (2001) 861–871. doi:doi.org/10.1006/jsvi.2000.3225.
[4] J. Ffowcs-Williams, Noise, anti-noise and flow control, Philosophical Transcations of the Royal Soc. A Matehmatical Physical Eng. Sci. 360 (2002) 821–832. doi:doi.org/10.1098/rsta.2001.0969.
[5] D. Crighton, A. Dowling, J. Ffowcs-Williams, M. Heckl, F. Leppington, Modern methods in analytical acoustics (Chapter 13. Thermoacoustic sources and instabilities) pp 378-405, Acoust. Soc. Am., 1992. doi:doi.org/10.1121/1.404334.
[6] A. P. Dowling, S. R. Stow, Acoustic analysis of gas turbine combustors, J. Propuls. Power 19 (2003) 751–764. doi:doi.org/10.2514/2.6192.
[7] K. McManus, T. Poinsot, S. Candel, A review of active control of combustion instabilities, Prog. Energy Combust. Sci. 19 (1993) 1–29. doi:doi.org/10.1016/0360-1285(93)90020-F.
[8] A. Annaswamy, M. Fleifil, J. Hathout, A. Ghoniem, Impact of linear coupling on the design of active controllers for the thermoacoustic instability, Combust. Sci. Technol. 128 (1997) 131–180. doi:doi.org/10.1080/00102209708935707.
[9] S. Candel, Combustion dynamics and control: progress and challenges, Proc. Combust. Inst. 29 (2002) 1–28. doi:doi.org/10.1016/S1540-7489(02)80007-4.
[10] A. Dowling, A. Morgans, Feedback control of combustion instabilities, Annu. Rev. Fluid Mech. 37 (2005) 151–182. doi:doi.org/10.1146/annurev.fluid.36.050802.122038.
[11] A. S. Morgans, S. R. Stow, Model-based control of combustion instabilities in annular combustors, Combust. Flame 150 (4) (2007) 380–399. doi:doi.org/10.1016/j.combustflame.2007.06.002.
[12] L. Crocco, Aspects of combustion instability in liquid propellant rocket motors. Part I., J. Am. Rocket Soc. 21 (1951) 163–178. doi:doi.org/10.2514/8.4393.
[13] L. Crocco, Aspects of combustion instability in liquid propellant rocket motors. part II., J. Am. Rocket Soc. 22 (1952) 7–16. doi:doi.org/10.2514/8.4410.
[14] H. Tsien, Servo-stabilization of combustion in rocket engines, J. Am. Rocket Soc. 22 (256–263) (1952). doi:doi.org/10.2514/8.4488.
[15] F. E. Marble, D. W. Cox Jr, Servo-stabilization of low frequency oscillations in bipropellant rocket motor, J. Am. Rocket Soc. 23 (63–74) (1953). doi:doi.org/10.2514/8.4542.
[16] L. Crocco, S. Cheng, Theory of combustion instability in liquid propellant rocket motors, Butterworths Scientific Publications, New York, 1956.
[17] D. J. Harrje, F. H. Reardon, Liquid propellant rocket instability, Tech. rep., NASA, Report SP-194 (1972).
[18] V. Yang, W. Anderson, Liquid Rocket Engine Combustion Instability, Am. Inst. Aeronaut. Astronaut., 1995.
[19] G. A. Richards, M. C. Janus, Characterization of oscillations during premix gas turbine combustion, J. Eng. Gas Turbines Power 120 (1998) 294–302. doi:doi.org/10.1115/1.2818120.
[20] T. Lieuwen, B. T. Zinn, The role of equivalence ratio oscillations in driving combustion instabilities in low nox gas turbines, Proc. Combust. Inst. 27 (1998) 1809–1816. doi:doi.org/10.1016/S0082-0784(98)80022-2.

[21] T. Lieuwen, H. Torres, C. Johnson, B. T. Zinn, A mechanism of combustion instability in lean premixed gas turbine combustors, J. Eng. Gas Turbines Power 123 (2001) 182–189. doi:doi.org/10.1115/1.1339002.
[22] S. Hubbard, A. Dowling, Acoustic resonances of an industrial gas turbine combustion system, J. Eng. Gas Turbines Power 123 (2001) 766–773. doi:doi.org/10.1115/1.1370975.
[23] C. O. Paschereit, W. Polifke, B. Schuermans, O. Mattson, Measurement of transfer matrices and source terms of premixed flames, J. Eng. Gas Turbines Power 124 (2002) 239–247. doi:doi.org/10.1115/1.1383255.
[24] T. C. Lieuwen, V. Yang, Combustion instabilities in gas turbines, Operational experience, Fundamental mechanisms, and Modeling, Progress in Astronautics and Aeronautics, Am. Inst. of Aeronaut. and Astronaut., Inc., 2005.
[25] K.-U. Schildmacher, R. Koch, H.-J. Bauer, Experimental characterization of premixed flame instabilities of a model gas turbine burner, Flow, Turbul. Combust. 76 (2006) 177–197. doi:doi.org/10.1007/s10494-006-9012-z.
[26] Y. Huang, V. Yang, Dynamics and stability of lean-premixed swirl-stabilized combustion, Prog. Energy Combust. Sci. 35 (2009) 293–384. doi:doi.org/10.1016/j.pecs.2009.01.002.
[27] W. Krebs, H. Krediet, E. Portillo, S. Hermeth, T. Poinsot, S. Schimek, C. Paschereit, Comparison of nonlinear to linear thermoacoustic stability analysis of a gas turbine combustion system, J. Eng. Gas Turbines Power 135 (2013) 081503. doi:doi.org/10.1115/1.4023887.
[28] S. Candel, D. Durox, T. Schuller, J.-F. Bourgouin, J. P. Moeck, Dynamics of swirling flames, Annu. Rev. Fluid Mech. 46 (2014) 147–173. doi:doi.org/10.1146/annurev-fluid-010313-141300.
[29] T. Poinsot, Prediction and control of combustion instabilities in real engines, Proc. Combust. Inst. 36 (2017) 1–28. doi:doi.org/10.1016/j.proci.2016.05.007.
[30] S. Candel, Combustion dynamics and control: Progress and challenges, Proc. Combust. Inst. 29 (2002) 1–28. doi:doi.org/10.1016/S1540-7489(02)80007-4.
[31] W. Polifke, Modeling and analysis of premixed flame dynamics by means of distributed time delays, Prog. Energy Combust. Sci. 79 (2020). doi:doi.org/10.1016/j.pecs.2020.100845.
[32] T. Schuller, T. Poinsot, S. Candel, Dynamics and control of premixed combustion systems based on flame transfer and describing functions, J. Fluid Mech. 894 (2020) 1–95. doi:doi.org/10.1017/jfm.2020.239.
[33] Y. Matsui, An experimental study on pyro-acoustic amplification of premixed laminar flames, Combust. Flame 43 (1981) 199–209. doi:doi.org/10.1016/0010-2180(81)90017-1.
[34] M. Fleifil, A. Annaswamy, Z. Ghoneim, A. Ghoniem, Response of a laminar premixed flame to flow oscillations: a kinematic model and thermoacoustic instability results, Combust. Flame 106 (1996) 487–510. doi:doi.org/10.1016/0010-2180(96)00049-1.
[35] S. Ducruix, D. Durox, S. Candel, Theoretical and experimental determinations of the transfer function of a laminar premixed flame, Proc. Combust. Inst. 28 (2000) 765–773. doi:doi.org/10.1016/S0082-0784(00)80279-9.
[36] T. Schuller, S. Ducruix, D. Durox, S. Candel, Modeling tools for the prediction of premixed Flame Transfer Functions, Proc. Combust. Inst. 29 (2002) 107–113. doi:doi.org/10.1016/S1540-7489(02)80018-9.
[37] T. Schuller, D. Durox, S. Candel, A unified model for the prediction of laminar flame transfer functions : comparisons between conical and V-flame dynamics, Combust. Flame 134 (2003) 21–34. doi:doi.org/10.1016/S0010-2180(03)00042-7.
[38] T. Lieuwen, Modeling premixed combustion-acoustic wave interactions: A review, J. Propuls. Power 19 (2003) 765–779. doi:doi.org/10.2514/2.6193.
[39] Preetham, T. Kumar, T. Lieuwen, Response of premixed flames to flow oscillations : unsteady curvature effects, Am. Inst. Aeronaut. Astronaut. Paper 2006-0960 (2006). doi:doi.org/10.2514/6.2006-960.
[40] Preetham, H. Santosh, T. Lieuwen, Dynamics of laminar premixed flames forced by harmonic velocity disturbances, J. Propuls. Power 24 (2008) 1390–1402. doi:doi.org/10.2514/1.35432.
[41] P. Palies, T. Schuller, D. Durox, S. Candel, Modeling of swirling flames transfer functions, Proc. Combust. Inst. 33 (2011) 2967–2974. doi:doi.org/10.1016/j.proci.2010.06.059.
[42] K. T. Kim, D. A. Santavicca, Generalization of turbulent swirl flame transfer functions in gas turbine combustors, Combust. Sci. Technol. 185 (2013) 999–1015. doi:doi.org/10.1080/00102202.2012.752734.
[43] V. N. Kornilov, M. Manohar, L. P. H. De Goey, Thermo-acoustic behavior of multiple flame burner decks : transfer function decomposition, Proc. Combust. Inst. 32 (2009) 1383–1390. doi:doi.org/10.1016/j.proci.2008.05.022.
[44] A. P. Dowling, Nonlinear self-excited oscillations of a ducted flame, J. Fluid Mech. 346 (1997) 271–290. doi:doi.org/10.1017/S0022112097006484.
[45] N. Noiray, D. Durox, T. Schuller, S. Candel, A unified framework for nonlinear combustion instability analysis based on the flame describing function, J. Fluid Mech. 615 (2008) 139–167. doi:doi.org/10.1017/S0022112008003613.
[46] D. Durox, T. Schuller, N. Noiray, S. Candel, Experimental analysis of nonlinear flame transfer functions for different flame geometries, Proc. Combust. Inst. 32 (2009) 1391–1398. doi:doi.org/10.1016/j.proci.2008.06.204.
[47] N. Noiray, D. Durox, T. Schuller, S. Candel, A method for estimating the noise level of unstable combustion based on the flame describing function, Intl. J. Aeroacoust. 8 (2009) 157–176. doi:doi.org/10.1260/147547209786234957.
[48] F. Boudy, D. Durox, T. Schuller, S. Candel, Nonlinear mode triggering in a multiple flame combustor, Proc. Combust. Inst. 33 (2011) 1121–1128. doi:doi.org/10.1016/j.proci.2010.05.079.
[49] F. Boudy, D. Durox, T. Schuller, G. Jomaas, S. Candel, Describing function analysis of limit cycles in a multiple flame combustor, J. Eng. Gas Turbines Power 133 (2011) 061502. doi:doi.org/10.1115/1.4002275.
[50] P. Palies, D. Durox, T. Schuller, S. Candel, Nonlinear combustion instability analysis based on the flame describing function applied to turbulent premixed swirling flames, Combust. Flame 158 (2011) 1980 – 1991.
[51] M. Heckl, Analytical model of nonlinear thermo-acoustic effects in a matrix burner, J. Sound Vib. 332 (2013) 4021–4036. doi:doi.org/10.1016/j.jsv.2012.11.010.
[52] C. Silva, F. Nicoud, T. Schuller, D. Durox, S. Candel, Combining a Helmholtz solver with the flame de-

scribing function to assess combustion instability in a premixed swirled combustor, Combust. Flame 160 (2013). doi:doi.org/10.1016/j.combustflame.2013.03.020.
[53] X. Han, A. Morgans, Simulation of the flame describing function of a turbulent premixed flame using an open-source LES solver 162 (2015) 1778–1792. doi:doi.org/10.1016/j.combustflame.2014.11.039.
[54] X. Han, J. Li, A. Morgans, Prediction of combustion instability limit cycle oscillations by combining flame describing function simulations with a thermoacoustic network model, Combust. Flame 162 (2015) 3632–3647. doi:doi.org/10.1016/j.combustflame.2015.06.020.
[55] M. Heckl, A new perspective on the flame describing function of a matrix flame, International Journal of Spray and Combustion Dynamics 7 (2015) 91–112. doi:doi.org/10.1260/1756-8277.7.2.91.
[56] S. Gopinathan, D. Iurashev, A. Bigongiari, M. Heckl, Nonlinear analytical flame models with amplitude-dependent time-lag distributions, International Journal of Spray and Combustion Dynamics 10 (2018) 264–276. doi:doi.org/10.1177/1756827717728056.
[57] G. Ghirardo, M. P. Juniper, J. P. Moeck, Weakly nonlinear analysis of thermoacoustic instabilities in annular combustors, J. Fluid Mech. 805 (2016) 52–87. doi:doi.org/10.1017/jfm.2016.494.
[58] D. Laera, T. Schuller, K. Prieur, D. Durox, S. M. Camporeale, S. Candel, Flame describing function analysis of spinning and standing modes in an annular combustor and comparison with experiments, Combust. Flame 184 (2017) 136–152. doi:doi.org/10.1016/j.combustflame.2017.05.021.
[59] M. Haeringer, M. Merk, W. Polifke, Inclusion of higher harmonics in the flame describing function for predicting limit cycles of self-excited combustion instabilities, Proc. Combust. Inst. 37 (2019) 5255–5262. doi:doi.org/10.1016/j.proci.2018.06.150.
[60] P. Rajendram Soundararajan, G. Vignat, D. Durox, A. Renaud, S. Candel, Effect of different fuels on combustion instabilities in an annular combustor, J. Eng. Gas Turb. Power 143 (2021) 031007. doi:doi.org/10.1115/1.4049702.
[61] G. Vignat, P. Rajendram Soundararajan, D. Durox, A. Vié, A. Renaud, S. Candel, A joint experimental and LES characterization of the liquid fuel spray in a swirl injector, J. Eng. Gas Turb. Power 143 (2021). doi:doi.org/10.1115/1.4049771.
[62] A. F. Seybert, D. F. Ross, Experimental determination of acoustic properties using a two-microphone random-excitation technique, J. Acoust. Soc. Am. 61 (1977) 1362–1370. doi:doi.org/10.1121/1.381403.
[63] P. Rajendram Soundararajan, D. Durox, A. Renaud, G. Vignat, S. Candel, Swirler effects on combustion instabilities analyzed with measured FDFs, injector impedances and damping rates, Under review in Combust. Flame (2021).
[64] A. Degenève, R. Vicquelin, C. Mirat, B. Labegorre, P. Jourdaine, J. Caudal, T. Schuller, Scaling relations for the length of coaxial oxy-flames with and without swirl, Proc. Combust. Inst. 37 (2019) 4563–4570. doi:doi.org/10.1016/j.proci.2018.06.032.
[65] M. Gatti, R. Gaudron, C. Mirat, L. Zimmer, T. Schuller, Impact of swirl and bluff-body on the transfer function of premixed flames, Proc. Combust. Inst. 37 (2019) 5197–5204. doi:doi.org/10.1016/j.proci.2018.06.148.
[66] G. Wang, T. F. Guiberti, X. Xia, L. Li, X. Liu, W. L. Roberts, F. Qi, Decomposition of swirling flame transfer function in the complex space, Combust. Flame 228 (2021) 29–41. doi:doi.org/10.1016/j.combustflame.2021.01.032.
[67] R. Gaudron, M. Gatti, C. Mirat, T. Schuller, Flame describing functions of a confined premixed swirled combustor with upstream and downstream forcing, J. Eng. Gas Turbines Power 141 (2019) 051016. doi:doi.org/10.1115/1.4041000.